

A tris-phenylphenol N₈O₃ Schiff-base cryptand: structural characterization and fluorescence titration for lanthanide coordination

Shu-Yan Yu,^{1*} Biao Wu,² Xiao-Juan Yang,³ Wen-Jian Zhang,² Xintao Wu² and Takahiro Kusukawa¹

¹Coordination Chemistry Laboratory, Institute for Molecular Science, Myodaiji, Okazaki 444, Japan

²Fujian Institute of Research on the Structure of Matter, Fujian 350002, China

³Department of Chemistry, Fuzhou University, Fujian 350002, China

Received 30 January 1998; revised 6 March 1998; accepted 6 March 1998

ABSTRACT: Lanthanide [lanthanum(III), **2**; europium(III), **3**; and gadolinium(III), **4**] cryptates of a tris-phenylphenol N₈O₃ Schiff-base cryptand (H₃L) were synthesized by transmetallation with [Na(H₃L)]ClO₄·3H₂O (**1**) and characterized by spectroscopic and crystal structure analyses. Both **3** and **4** are isomorphous and isostructural. The complexes crystallize in the triclinic space group *P*-1 with cell parameters for **3** of *a* = 14.9833(2), *b* = 15.42670(10), *c* = 16.3770(3) Å, α = 75.3760(10), β = 68.2640(10), γ = 77.0540(10)° and *Z* = 2 and for **4** of *a* = 14.9976(3), *b* = 15.4417(3), *c* = 16.35350(10) Å, α = 75.4980(10), β = 68.3180(10), γ = 76.8790(10)° and *Z* = 2. The structures reveal that one lanthanide ion is unsymmetrically encapsulated in the cryptand cavity with a second ligand (solvent DMF). Solution NMR and solid structural studies demonstrated that there are intracavity and intermolecular proton transfer processes during lanthanide complexation towards the cryptand. A fluorimetric titration in acetonitrile for Eu(III) ion to **1** afforded a novel fluorescence intensity (*I_F*)–equivalents of Eu(III) ion (*x*) plot signaling a quenching (0 < *x* < 0.2)–enhancement (0.2 < *x* < 1) change with formation of the kinetically stable 1:1 cryptate. An energy-transfer mechanism is discussed. © 1998 John Wiley & Sons, Ltd.

KEYWORDS: cryptand; fluorescence titration; lanthanide coordination; proton transfer

INTRODUCTION

Lanthanide complexes are of increasing interest in supramolecular chemistry, biology and medicine. For example, luminescent Eu³⁺ and Tb³⁺ complexes with encapsulating ligands have been extensively studied as potential molecular and supramolecular devices,¹ fluorescent probes and luminescent labels in biological systems and medical diagnostics.^{2,3} Gd³⁺ complexes are possible contrast-enhancing agents for magnetic resonance imaging.^{4,5} Recently, lanthanide complexes have been used as catalysts for the hydrolysis of phosphodiester and of DNA.^{6–8} We have reported the use of lanthanide complexes to scavenge superoxide radicals.⁹ To form more stable lanthanide complexes for further potential use, the design and syntheses of macrocyclic lanthanide complexes are currently attracting much attention.¹⁰ Recently, we have studied the syntheses and characterization of kinetically stable lanthanide complexes of an N₈O₃ Schiff-base cryptand

derived from a 2 + 3 condensation of tris(2-aminoethyl)-amine and 2,6-diformyl-4-methoxyphenol.^{11,12} As a further approach to a potential fluorescent chemosensor,^{13,14} we synthesized a novel analogue, H₃L (Fig. 1), in which three fluorescent phenylphenol units have been incorporated, and we describe here its structural characterization and spectroscopic properties for lanthanide coordination. Moreover, a novel profile of fluorescence intensity–metal equivalents was obtained through a spectrofluorimetric titration for Eu³⁺ ion complexation.

RESULTS AND DISCUSSION

Structures of cryptates **3** and **4**

Crystals of both **3** and **4** are isomorphous, possessing the general formula [Ln(H₂L)(DMF)](ClO₄)₂·*n*H₂O·0.5Et₂O (where Ln = Eu, *n* = 2 in **3** and Gd, *n* = 6 in **4**). The structures of both cationic cryptates [Eu(H₂L)(DMF)]²⁺ in **3** and [Gd(H₂L)(DMF)]²⁺ in **4** are isostructural with each other, as shown in Figs 2 and 3. Selected bond lengths and angles are listed in Table 1.

The complexes crystallize in the triclinic *P*-1 space group. In the cationic cryptate [Eu(H₂L)(DMF)]²⁺, the

*Correspondence to: S.-Y. Yu, Coordination Chemistry Laboratory, Institute for Molecular Science, Myodaiji, Okazaki 444, Japan.
Email: ysy@ims.ac.jp

Contract/grant sponsor: State Key Laboratories of Coordination Chemistry (Nanjing University) and Structural Chemistry (FJIRSM).

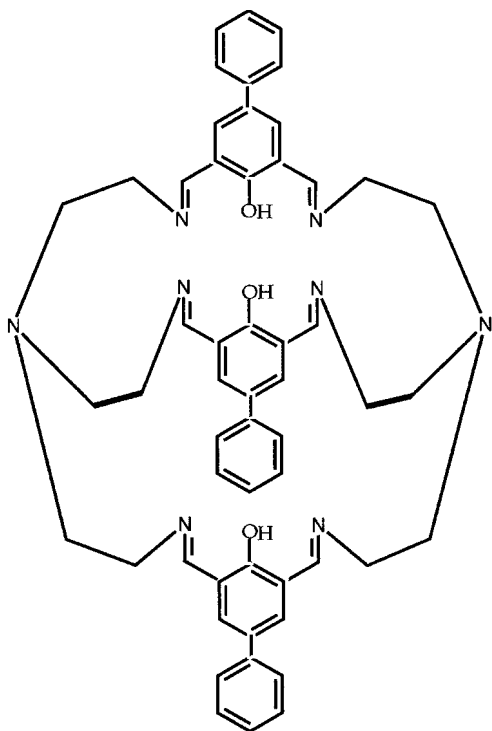


Figure 1. Tris-phenylphenol cryptand H_3L

Eu^{3+} ion coordination with the deprotonated two-proton cryptand is similar to those of the Eu^{3+} cryptates described in a previous paper,¹¹ i.e. the Eu atom has an eight-coordinate environment consisting of an N_4O_3 donor-set from the cryptand cavity and a second-donor O from a DMF solvent molecule. One metal ion is placed unsymmetrically at one site of the cryptand cavity, in which the remaining N_4 donor-set may be empty or act as a host for protons transferred from the phenylphenol units. Although the tris-phenylphenol cryptand cavity is capable of functioning as 11 donors in symmetrical $N_4O_3N_4$ form to bind one or two metals, only one lanthanide ion is bound asymmetrically by seven donors (N_4O_3) from the cavity. The second lanthanide ion is unable to enter the empty chamber in the cavity. This is possibly attributable to the large radii and high coordinate numbers of lanthanide ions and the size and rigidity of the Schiff-base cryptand cavity. It seems impossible to obtain an f-f binuclear or a symmetrical mononuclear f complex of this kind of cryptand, although homo- and heterobinuclear transition metal complexes of this kind of cryptand were reported in 1985.¹⁵ Beyond the complexation inside the cavity, to meet the eight-ordination about the lanthanide ion, a second donor is always

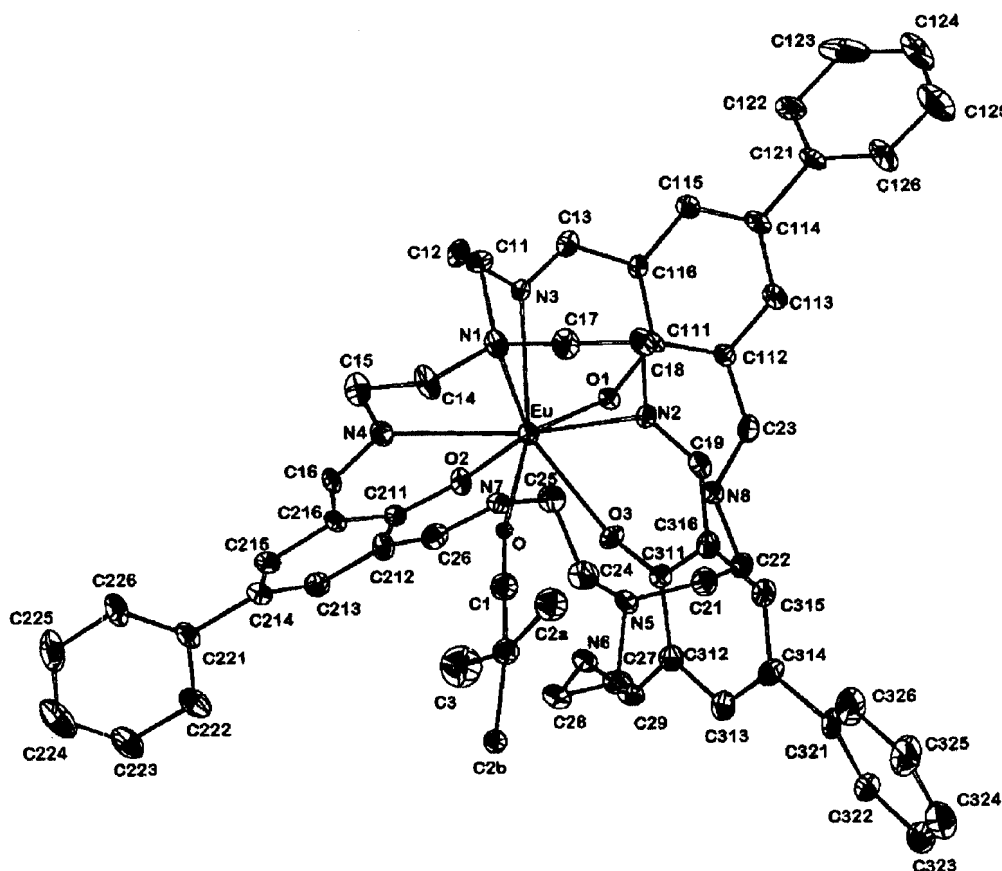


Figure 2. Structure of the cationic cryptate $[Eu(H_2L)(DMF)]^{2+}$ in **3** (H atoms omitted; thermal ellipsoids are shown at 20% probability)

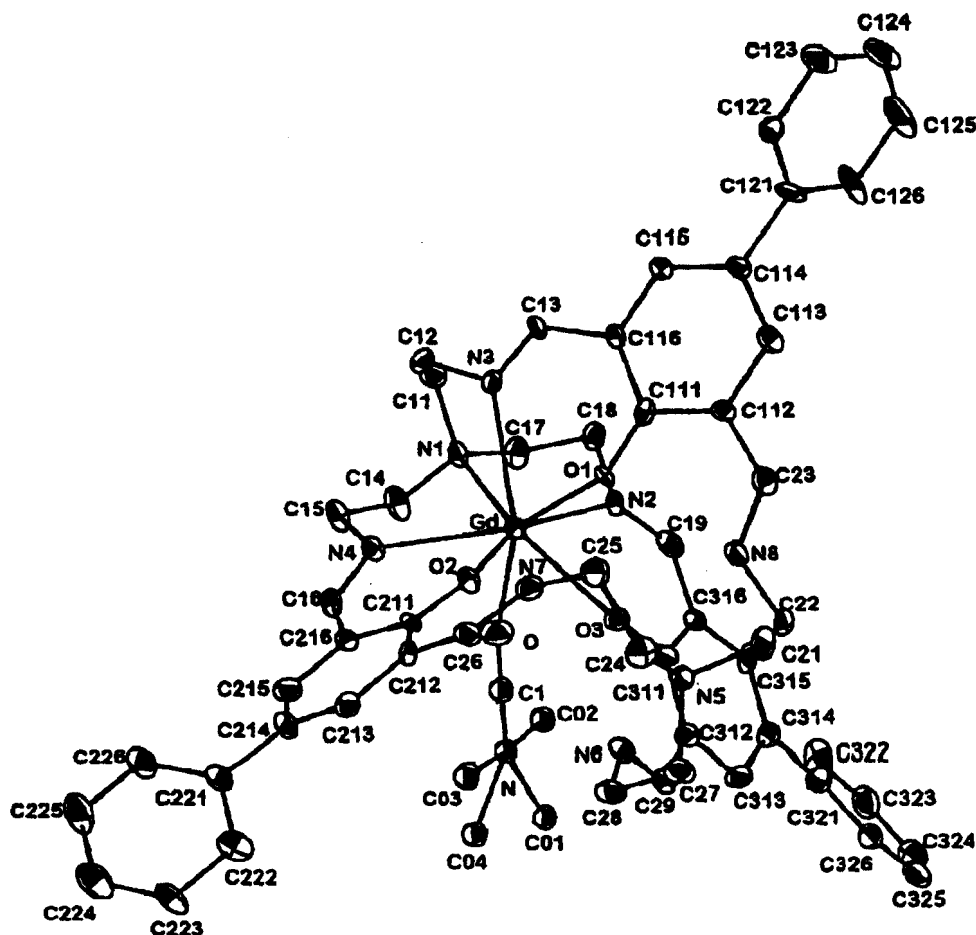


Figure 3. Structure of the cationic cryptate $[\text{Gd}(\text{H}_2\text{L})(\text{DMF})]^{2+}$ in **4** (H atoms omitted; thermal ellipsoids are shown at 20% probability)

present.^{11,12,16} It is noteworthy that the second donor is variable. In solution (acetonitrile mixed with a few drops of DMF), the second donor may come from water, acetonitrile and DMF molecules. Owing to the strong binding potential with lanthanides, an oxygen donor from a DMF molecule is dominantly bonded to an Eu ion in the remaining coordinate site to meet the eight-coordinate dodecahedron. The Eu—O distance of 2.343(11) Å is slightly shorter (by 0.1 Å) than that of Eu—O (water as the second donor),¹¹ showing the stronger binding between Eu and O donor from DMF. In the cavity, the three Eu—O (phenol) units have different bond distances, corresponding to inequivalent proton transfer from the three phenylphenols upon Eu^{3+} coordination. This is different from what occurred in a mononuclear Eu^{3+} complex with a 2 + 2 Schiff-base macrocyclic phenolate-bridged ligand,¹⁷ in which both Eu—O (phenol) bond lengths are equally short, 2.28(1) Å, showing that two protons have transferred from the corresponding phenolic oxy-

gens. In the cryptate **3**, the shortest Eu—O (phenol) bond, Eu—O(2) = 2.284(8) Å, agrees with that of the macrocyclic complex,¹⁷ regarded as bonding between Eu and the deprotonated phenol oxygen, while the other two are too long [2.346(8) and 2.370(8) Å], indicating that the remaining protons have partly transferred inside the cavity. It has been shown that proton transfer for the three phenylphenols in the cavity is non-equivalent and stepwise. Single-crystal analyses of the cryptates **3** and **4** reveal that one lanthanide cryptate cation matches two perchlorate anions together with crystalline neutral solvent molecules. Consequently, the cryptand receptor recognizes one lanthanide cationic guest in a deprotonated two-proton form (H_2L^-), suggesting that one phenylphenol OH in the cryptand has transferred into the solution. A coordination proton transfer may be described by the following equations, where S represents solvent acetonitrile or water coming from the hydrate lanthanide perchlorates:

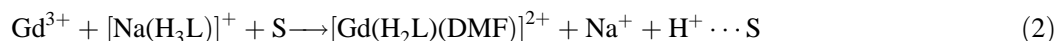
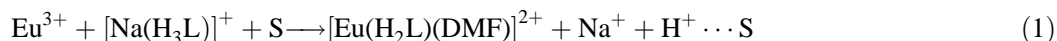


Table 1. Selected bond lengths (Å) and bond angles (°) for **3** and **4**

3		4	
Eu—O(1)	2.346(8)	Gd—O(1)	2.339(10)
Eu—O(2)	2.284(8)	Gd—O(2)	2.293(9)
Eu—O(3)	2.370(8)	Gd—O(3)	2.358(10)
Eu—O	2.343(11)	Gd—O	2.340(13)
Eu—N(1)	2.660(10)	Gd—N(1)	2.689(12)
Eu—N(2)	2.505(9)	Gd—N(2)	2.501(12)
Eu—N(3)	2.522(9)	Gd—N(3)	2.532(12)
Eu—N(4)	2.605(9)	Gd—N(4)	2.573(12)
O(2)—Eu—O	100.6(3)	O(2)—Gd—O	101.0(4)
O(2)—Eu—O(1)	80.0(3)	O(2)—Gd—O(1)	79.3(3)
O—Eu—O(1)	143.5(3)	O—Gd—O(1)	142.6(4)
O(2)—Eu—O(3)	83.1(3)	O(2)—Gd—O(3)	82.6(4)
O—Eu—O(3)	73.0(3)	O—Gd—O(3)	72.8(4)
O(1)—Eu—O(3)	70.8(3)	O(1)—Gd—O(3)	70.1(3)
O(2)—Eu—N(2)	155.2(3)	O(2)—Gd—N(2)	155.1(4)
O—Eu—N(2)	79.2(3)	O—Gd—N(2)	79.1(4)
O(1)—Eu—N(2)	85.7(3)	O(1)—Gd—N(2)	85.8(4)
O(3)—Eu—N(2)	73.1(3)	O(3)—Gd—N(2)	73.6(4)
O(2)—Eu—N(3)	101.2(3)	O(2)—Gd—N(3)	101.1(4)
O—Eu—N(3)	143.8(4)	O—Gd—N(3)	144.1(4)
O(1)—Eu—N(3)	69.2(3)	O(1)—Gd—N(3)	69.7(4)
O(3)—Eu—N(3)	138.2(3)	O(3)—Gd—N(3)	138.1(4)
N(2)—Eu—N(3)	92.3(3)	N(2)—Gd—N(3)	92.1(4)
O(2)—Eu—N(4)	71.8(3)	O(2)—Gd—N(4)	72.3(4)
O—Eu—N(4)	70.4(3)	O—Gd—N(4)	70.9(4)
O(1)—Eu—N(4)	140.5(3)	O(1)—Gd—N(4)	140.6(4)
O(3)—Eu—N(4)	130.2(3)	O(3)—Gd—N(4)	130.3(4)
N(2)—Eu—N(4)	129.5(3)	N(2)—Gd—N(4)	129.4(4)
N(3)—Eu—N(4)	89.5(3)	N(3)—Gd—N(4)	89.5(4)
O(2)—Eu—N(1)	135.9(3)	O(2)—Gd—N(1)	136.1(4)
O—Eu—N(1)	79.1(4)	O—Gd—N(1)	79.0(4)
O(1)—Eu—N(1)	125.6(3)	O(1)—Gd—N(1)	126.5(4)
O(3)—Eu—N(1)	136.0(3)	O(3)—Gd—N(1)	136.3(4)
N(2)—Eu—N(1)	68.7(3)	N(2)—Gd—N(1)	68.6(4)
N(3)—Eu—N(1)	65.1(3)	N(3)—Gd—N(1)	65.4(4)
N(4)—Eu—N(1)	66.7(3)	N(4)—Gd—N(1)	66.3(4)

Spectroscopy of the cryptates

All complexes present similar IR features. There is a very strong band at *ca* 1650 cm⁻¹ assigned to the imino C=N stretching vibration. The band at 1087–1097 cm⁻¹ is characteristic of the perchlorate anion. As for their UV–visible spectra in acetonitrile, the sodium cryptate [Na(H₃L)]ClO₄·3H₂O (**1**) exhibits three absorption bands at 284, 350, and 445 nm, whereas all lanthanide complexes, **2**, **3** and **4** (La³⁺, Eu³⁺ and Gd³⁺), present only two strong absorption bands at 293 and 415 nm. All absorption spectra are due to the π – π^* transition of the tris-phenylphenol moieties.

The sodium complex **1** and lanthanum complex **2** were characterized by chemical analyses and fast atom bombardment (FAB) mass and NMR spectra. The FAB mass spectra show that **1** has a base-ion peak at *m/z* 886 and a weak peak at *m/z* 863, corresponding to the monosodium cryptate [Na(H₃L)+1]⁺ and the metal-free cryptand [(H₃L)+1]⁺, respectively. In the FAB mass spectra of **2**, there are two important peaks at *m/z* 1100

and 1001, due to the species [La(H₃L)(ClO₄)]⁺ and [La(H₃L)]⁺, respectively, resulting from the loss of perchlorate and water. The peak corresponding to [La(H₃L)(H₂O)]⁺ was not found, possibly attributable to the weak binding between La and the second ligand H₂O. No peak assigned to the metal-free cryptand ligand was observed but the fragments resulting from the broken macrobicycle were. This confirms the high kinetic stability of lanthanide cryptates; similar cases have been reported recently by Avecilla *et al.*¹⁶

Like the other sodium cryptates of the N₈O₃ Schiff-base cryptands reported previously,^{11,12} **1** presents broad overlapped NMR spectra in DMSO-*d*₆ (or in CD₃CN or CDCl₃) at room temperature, possibly resulting from the conformational mobility or multiple-proton transfer in the cavity. Owing to the low solubility, it seems that the Schiff-base compound is difficult to use in further NMR studies. However, the lanthanum complex **2** has fair solubility in acetonitrile, DMF and DMSO. NMR experiments in CD₃CN give the same distinguishable unsymmetrical resonance mode as in our previous

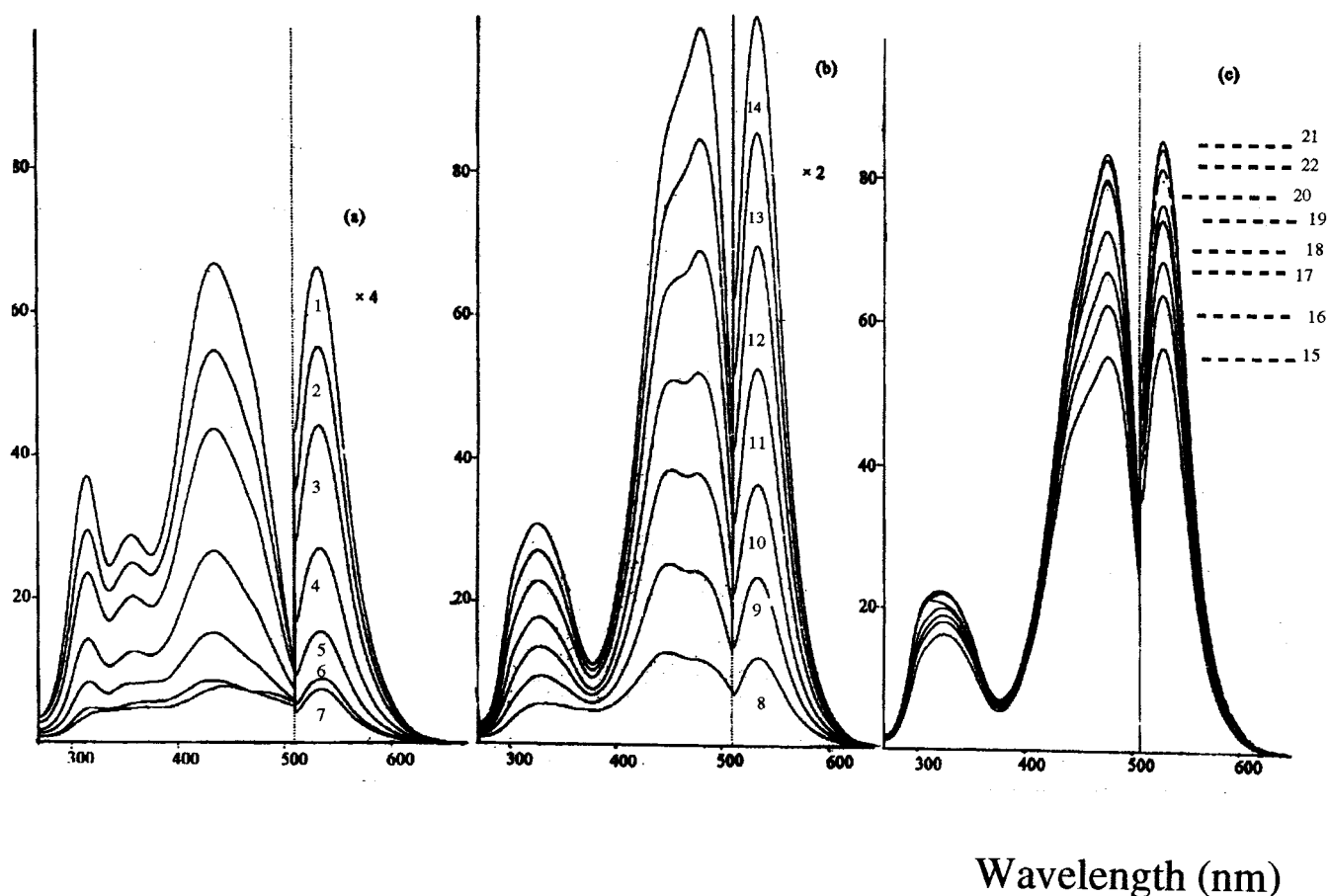
I_F 

Figure 4. Fluorescence spectra for Eu^{3+} titrations of **1** ($9.1 \times 10^{-5} \text{ mol dm}^{-3}$) in acetonitrile at room temperature. Left, excitation spectra; right, emission spectra. I_F is relative fluorescence intensity; x is equivalents of Eu^{3+} ion added. (a) Excitation at 436 nm, emission measured at 536 nm. $x = (1) 0; (2) 0.02; (3) 0.036; (4) 0.072; (5) 0.11; (6) 0.15; (7) 0.17$. (b) Excitation at 482 ± 2 nm, emission measured at 536 nm. $x = (8) 0.18; (9) 0.20; (10) 0.24; (11) 0.28; (12) 0.30; (13) 0.34; (14) 0.38$. (c) Excitation at 482 ± 2 nm, emission measured at 536 nm. $x = (15) 0.42; (16) 0.49; (17) 0.58; (18) 0.68; (19) 0.78; (20) 0.88; (21) 0.98; (22) 2.20$

observation for another lanthanide cryptate of a trisphenol N_8O_3 Schiff-base cryptand.¹¹ This mode suggests that only one metal ion is coordinated in one site of the cavity of the compartmental cryptand, in which another site is empty or serves as a host for protons, with similar unsymmetric compartmental coordination to the solid structures of **3** (Fig. 2) and **4** (Fig. 3). Hence the corresponding proton resonance splits into two pairs of peaks. For instance, the ^1H NMR spectrum of **2** displays two pairs of peaks at δ 8.71, 8.68 (doublet) and 8.50 (singlet) assigned to two kinds of imino protons ($\text{HC}=\text{N}$), and two pairs of resonances at δ 8.20, 8.19 (doublet, $J = 2.5$ Hz) and 8.02, 8.01 (doublet, $J = 2.5$ Hz), corresponding to the protons at the 3 and 5 sites of Ph(1), respectively. Also, the ^{13}C NMR and $^{13}\text{C}-\text{H}$ COSY data suggest two kinds of imino carbons at δ 173.00 and 169.08. It is noteworthy that there is a broad peak at δ 12.81 in the ^1H NMR spectrum, attributed to the three

phenylphenol OH protons. From $^1\text{H}-^1\text{H}$ COSY, this broad peak has a coupling at δ 8.71, 8.68 (doublet, $J = 15.0$ Hz), indicating that proton transfer occurred partially or completely from the phenylphenol oxygen to the imino nitrogen. The related imino group may be described as $^+\text{HN}=\text{CH}$ and the intracavity hydrogen bond as $\text{O}-\text{HN}^+$ forms.¹¹ In the opinion of AVECILLA *et al.*,¹⁶ it is difficult to decide whether one, two, three or none of the protons was transferred from the phenolic oxygen to the imino nitrogen under various conditions, because it is affected by many factors in solution. We have made some contrasting observations. In CD_3CN at room temperature, we obtain a clearly resolved spectrum in the low-field region for **2**. However, in $\text{DMSO}-d_6$ at the same temperature, the spectrum changed into a broad overlapped form. When an excess of La^{3+} ions was added to a solution of **2** in CD_3CN at room temperature, some important changes took place. The spectrum did not show

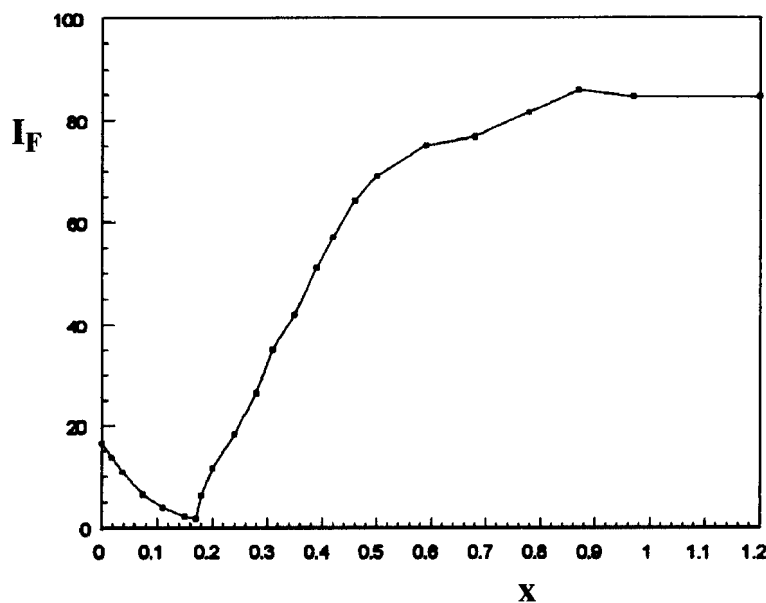


Figure 5. Fluorescence Eu^{3+} titrations of **1** in acetonitrile. I_F is relative fluorescence emission intensity ($\pm 2\%$); x denotes the equivalents of Eu^{3+} ion added to the solution of **1** (± 0.01)

the resonances for the three phenylphenol OH protons; moreover, the coupling at δ 8.71 (doublet) in the spectrum of **2** alone was reduced to a singlet at δ 8.69. These results might be explained by the three phenylphenol OH proton transfer being promoted by an excess of lanthanide ions. The resonances of the imino protons give two singlets at δ 8.69 and 8.45. Those of the phenyl Ph(1) protons retain two doublets at δ 8.15, 8.14 ($J = 2.5$ Hz) and 7.98, 7.97 ($J = 2.5$ Hz) related to 3-H and 5-H in Ph(1). These spectroscopic features still confirm the unsymmetrical mono-metal coordination in the cryptand cavity, whatever proton transfer occurs in the solution. We should state here that proton transfer may be affected by the radii and nature of the lanthanide ions. Also, the solution situation can be different from that in the solid state. Under the same reaction conditions, we obtained solid lanthanide cryptates with different proton states, such as $\text{La}(\text{H}_3\text{L})$ in **2**, $\text{Eu}(\text{H}_2\text{L})$ in **3** and $\text{Gd}(\text{H}_2\text{L})$ in **4**. Further, the three Ph(2) always show a symmetrical resonance mode, not affected by the unsymmetrical coordination inside the cavity.

Fluorescence titration for Eu^{3+} complexation

Fluorimetric titration for Eu^{3+} complexation in acetonitrile at room temperature gave the results shown in Fig. 4.

If non-luminescent La^{3+} or Gd^{3+} ion is added to a solution of **1** in acetonitrile, no change in the ligand fluorescence takes place. However, addition of luminescent Eu^{3+} ion to the system changes either the fluorescence intensity or the excitation wavelength. Only emission centered at 536 nm is observed during Eu^{3+} ion titrations for **1** and no lanthanide emission is sensitized. A

progressive decrease in the ligand fluorescence occurs in the region $0 < x < 0.2$ until quenching is maximum at x close to 0.2 [Fig. 4(a)]. The quenching may arise from an intermolecular process¹⁰ or the proton transfer from the phenolic oxygen to the solvent, as in the proposed process based on the crystal structure analysis for **3**. After the quenching point, the fluorescence emission is enhanced linearly ($0.2 < x < 0.5$). The fluorescence increases slowly ($0.5 < x < 0.9$) with Eu^{3+} titrations as shown in Fig. 4(b) and (c). The maximum appears at x near 0.9. Even if an excess of Eu^{3+} ion (x up to 2.20) is added to the system, the fluorescence is not altered, indicative of the formation of a unique 1:1 mononuclear complex. Moreover, even after the addition of non-luminescent La^{3+} or Gd^{3+} ion to the coordination-saturated fluorescent system, no fluorescence change is observed. This confirms the high kinetic stability of the Eu^{3+} cryptate in solution. The excitation spectra (left part of Fig. 4) show a similarity with the corresponding absorption. At $x = 0$, the spectra give three bands for the sodium complex **1** at 315, 360 and 436 nm, and similar absorption spectra are obtained with bands at 284, 350 and 445 nm in acetonitrile. At x near 0.9, the excitation spectra show two bands at 320 and 482 nm for the 1:1 Eu^{3+} cryptate; the corresponding absorption spectra for Eu^{3+} cryptate **3** also display two bands at 293 and 415 nm. The spectroscopic analogy indicates that fluorescence arises from the energy transfer^{18–20} from the chromophoric phenylphenol units to the bound Eu^{3+} . The total fluorescence Eu^{3+} titration of the tris-phenylphenol cryptand gives a novel profile for relative fluorescence intensity (I_F) versus equivalents of Eu^{3+} ion added (x) (Fig. 5).

Three turning points in the profile occurred at $x = 0, 0.2$ (-0.02) and 0.9 (-0.02), corresponding to ligand

emission, fluorescence quenching, and maximum enhancement with 1:1 complex formation, respectively. The plot may be relevant to the stepwise proton transfer for the three phenylphenol protons in the cryptand with Eu^{3+} complexation. In the case of the Tb^{3+} complex of calix[4]arene ligand (which bears four phenols),¹⁸ the fluorescence intensity is pH dependent. The trisphenylphenol cryptand should exhibit similar fluorescence intensity changes with the stepwise proton transfer upon lanthanide coordination. However, owing to the poor solubility, further studies of pH-dependent fluorescence Eu^{3+} ion titration for the Schiff-base cryptand have not yet been performed.

The contribution of the directly excited tris-phenylphenol cryptand ($x=0$, $\lambda_{\text{exc}}=436$ nm) to the fluorescence was found to be a small fraction ($I_{\text{F}}=17\%$), but the maximum I_{F} of 86% occurred at x near 0.9. According to our experiments, complexation towards non-photoactive metal ions (La^{3+} , Gd^{3+} and Na^{+}) does not enhance the ligand fluorescence. Therefore, we consider that the fluorescence signal changes may not result from metal complexation or from the proton transfer in the cavity. It may be interpreted by a similar energy-transfer mechanism to that described by Sato *et al.*¹⁸ for luminescent lanthanide complexes with water-soluble calix[4]arenes bearing four phenols. According to the energy level diagrams for Eu^{3+} calix[4]arene complexes,^{19,20} energy transfer from the simple phenol units to bound Eu^{3+} is extremely difficult, owing to the charge-transfer band (near 300 nm) which deactivates the excited state of the phenol unit to the ground state. We observed that the Eu^{3+} cryptate of a trisphenol cryptand showed a very weak ligand emission at 525 nm (excited at 300 nm).¹¹ However, after introduction of the phenyls to the cryptand, the fluorescence of the Eu^{3+} cryptate is apparently enhanced over four-fold. This shows that the sensitizer-to-metal energy transfer is essential to this system. The energy transfer may occur from the triplet level ($^3\pi\pi^*$) of the phenylphenol sensitizer to the 5D_0 emission level of the Eu^{3+} cryptate. The sensitized metal emission is centered at *ca* 614 nm.^{2,19} However, we did not observe the emission, possibly quenched by the coordinated solvent-like water molecule. The Horrocks–Sudnick equation²¹ proves that the rate constant for non-radiative energy transfer to the OH vibrational manifold of OH oscillators (e.g. coordinated water molecules) is significant for the Eu^{3+} ion. It is possible to quench the Eu^{3+} emission within one water molecule coordination towards the Eu^{3+} center in the cryptate. The x-ray crystal structure of the Eu^{3+} cryptate **3** reveals that an Eu^{3+} ion is unsymmetrically coordinated by the N_4O_3 donor set of the cryptand cavity. This represents less effective encapsulation for the lanthanide ion than with the eight-coordinate lanthanide complexes of calix[4]arenes,¹⁸ although they have similar phenolic oxygen donors. To meet the eight-coordination around the Eu^{3+} ion, a second donor is needed, hence the solvent water from the

hydrate Eu^{3+} perchlorate in this titration system may bind Eu^{3+} ion in the remaining site, resulting in metal emission quenching.

CONCLUSIONS

Being interested in novel physical and chemical properties of and potential uses in materials and biological systems of f-block lanthanides, we designed and synthesized the fluorescent tris-phenylphenol cryptand H_3L and resulting kinetically stable lanthanide cryptates. The NMR and FAB mass spectra characterized **1** as possessing a three-proton cryptand ligand H_3L . Based on NMR studies of the diamagnetic La^{3+} cryptate **2**, we discussed the solution proton transfer in the cryptand cavity. The proton transfer occurred only inside the cavity if an equivalent of La^{3+} ions complexed with the cryptand. Addition of an excess of La^{3+} ions cannot produce complexation but promotes the proton transfer from the phenol OH to solvents (such as water) outside the cryptand cavity. Crystal structural analyses revealed that solid complexes **3** and **4** have another proton state in the cryptand ligand cavity, in which one proton is transferred from the phenolic oxygen to the solvent, leading to a crystalline complex with the formula $[\text{Ln}(\text{H}_2\text{L})(\text{DMF})](\text{ClO}_4)_2 \cdot n\text{H}_2\text{O} \cdot 0.5\text{Et}_2\text{O}$. This indicates there are two different proton transfer processes accompanying lanthanide complexation, one intracavity and the other intermolecular proton transfer. Even if intracavity proton transfer occurred, it is not equivalent for the three phenylphenol protons. Therefore, we observed multiple fluorescence changes during the fluorimetric Eu^{3+} titrations of the cryptand. Furthermore, an important conclusion is the spectroscopically and structurally proved high kinetic stabilities of the 1:1 lanthanide complexes resulting from the unsymmetrical recognition of the compartmental cryptand toward lanthanide ions. The fluorescence emission involves a sensitizer-to-metal energy-transfer mechanism by photo-active Eu^{3+} bonding with the three fluorescent phenylphenolic oxygen donors and resulting proton transfer. We may consider the supramolecular system as a fluorescent chmosensor operating via pM and pH.^{13,14}

EXPERIMENTAL

General methods. All chemicals were prepared by previously reported methods.¹¹ All solvents used in syntheses were commercial products and were used without further purification. 2,6-Diformal-4-phenylphenol was synthesized in 45% yield as yellow crystals with satisfactory elemental analysis (Analysis: calculated for $\text{C}_{14}\text{H}_{10}\text{O}_3$, C 74.34, H 4.42; found, C 74.53, H 4.45%) and ^1H NMR spectra (500 MHz, CDCl_3): 11.63 (s, 1 H, phenol); 10.32 (s, 2 H, CHO); 8.20 [s, 2 H, Ph(1)–H(3,5)];

Table 2. Crystallographic data for the cryptates **3** and **4**

Parameter	3	4
Formula	C ₅₉ H ₆₉ Cl ₂ EuN ₉ O _{14.5}	C ₅₉ H ₇₇ Cl ₂ GdN ₉ O ^{18.5}
Formula weight	1359.12	1436.47
<i>F</i> (000)	1372	1476
Space group	<i>P</i> -1	<i>P</i> -1
<i>a</i> (Å)	14.9833(2)	14.9976(3)
<i>b</i> (Å)	15.42670(10)	15.4417(3)
<i>c</i> (Å)	16.3770(3)	16.35350(10)
α (°)	75.3760(10)	75.4980(10)
β (°)	68.2640(10)	68.3180(10)
γ (°)	77.0540(10)	76.8790(10)
<i>V</i> (Å ³)	3366.30(8)	3368.91(10)
<i>Z</i>	2	2
<i>D</i> _c (g cm ⁻³)	1.341	1.416
μ (cm ⁻¹)	1.076	1.137
Approx. crystal size (mm)	0.10 × 0.20 × 0.15	0.10 × 0.20 × 0.18
Radiation, λ (Å)	Mo K α (0.71073)	Mo K α (0.71073)
Temperature (K)	293 ± 2	293 ± 2
Scan type	ω	ω
Range of 2θ (°)	3.28–46.58	3.30–46.50
Range of <i>hkl</i>	–16/16, –11/17, –15/18	–16/12, –17/15, –18/16
No. of total reflections	9387	9393
No. of observed reflections	6795 with <i>I</i> > 2 σ	7195 with <i>I</i> > 2 σ
No. of refined parameters	676	754
<i>R</i> (obs./total)	0.0924/0.1249	0.1043/0.1448
<i>wR</i> (obs./total)	0.2475/0.2754	0.2355/0.2845
Goodness of fit (obs./total)	1.116/1.053	1.162/1.223
Final $\Delta\rho_{\max}/\Delta\rho_{\min}$ (e Å ⁻³)	1.756/–1.578	1.512/–0.968
	$w = 1/[\sigma^2(F_0^2) + (0.1793P)^2 + 3.5053P]$	$w = 1/[\sigma^2(F_0^2) + (0.0778P^2 + 72.0901P)]$

^a $P = (F_0^2 + 2F_0^2)/3$.

7.60 [d, 2 H, Ph(2)–H(2',6')]; 7.50, 7.48, 7.47 [t, 2 H, Ph(2)–(3',5')]; 7.42 [m, 1 H, Ph(2)–(4')]; ³*J*_{HH} = 7.5 Hz in Ph(2).

Spectra. NMR spectra were measured on a Varian Unity 500 spectrometer at room temperature with SiMe₄ as internal standard. FAB mass spectra were obtained on a Finnigan MAT 8430 spectrometer with *m*-nitrobenzyl alcohol as the matrix. IR spectra were recorded on a Perkin-Elmer 577 spectrophotometer in the range 4000–400 cm⁻¹ (KBr pellets). UV–Visible spectra were recorded on a Shimadzu UV-3000 spectrophotometer at room temperature from *ca* 10⁻⁵ mol dm⁻³ acetonitrile solution. Fluorescence titration was performed on a Shimadzu RF-540 spectrophotometer in acetonitrile at 295 K. The solvent acetonitrile used in spectroscopic studies was distilled from P₂O₅. To a solution of the sodium cryptate **1** in acetonitrile (9.1 × 10⁻⁵ mol dm⁻³) were added a solution of Eu(ClO₄)₃·6H₂O in acetonitrile (8.4 × 10⁻⁴ mol dm⁻³). In Eu³⁺ ion titrations, the maximum excitation wavelength changed (0 < *x* < 0.2, excitation at 436 nm; 0.2 < *x* < 2.20, excitation at 482 ± 2 nm). Emission was centered at 536 nm. The slit width was 5 nm. The spectra were corrected for the sensitivity.

X-ray crystallographic study. Crystallographic data are given in Table 2. Yellow block crystals of **3** and **4** were obtained by slow diffusion of diethyl ether into the

acetonitrile solution mixed with a few drops of DMF. Both are isomorphous and isostructural. Data were collected on a Siemens SMART CCD area-detector diffractometer and corrected for absorption by SADABS.²² A total of 1261 frames were collected with a graphite monochromator in a three-cycle goniometer. All calculations were performed on a INDY workstation using the SHELXL 93 program package.²³ Some atoms set in the second-ligand DMF and in the benene ring Ph(2) and also the crystalline solvents are disordered. The terminal C atoms in the second-ligand DMF have 50% occupation, such as C(2a) and C(2b) for **3** and C(01), C(02), C(03) and C(04) for **4**.

[Na(H₃L)]ClO₄·3H₂O (**1**). To a mixture of an excess of NaClO₄ (0.50 g, over 4 mmol) and 2,6-diformyl-4-phenylphenol (0.339 g, 1.5 mmol) in anhydrous methanol (50 cm³) was added dropwise an anhydrous methanol solution (50 cm³) of tris(2-aminoethyl)amine (0.146 g, 1 mmol). After stirring for 1 h at room temperature, the resulting yellow precipitate of **1** was isolated, washed with methanol and dried over CaCl₂, yield 0.41 g (79%). IR (KBr), ν = 3429w, 3057, 3030, 2939, 2837, 1649vs (CN), 1598, 1521, 1452, 1408, 1344, 1276, 1219, 1157, 1097s (ClO₄⁻), 885, 761, 698, 623, 607 cm⁻¹; UV–visible (acetonitrile), λ_{\max} (log ϵ) = 284 (4.26), 350 (2.76), 445 (3.61); ¹H NMR (500 MHz, DMSO-*d*₆),

$\delta = 13.58$ (br, 3 H, phenol-OH), 9.19 (br, 6 H HC=N), 8.33 [br, 6 H, Ph(1)H], 7.47 [m, 15 H, Ph(2)H], 3.70–2.99 (m, 24 H, CH₂CH₂); FAB-MS, m/z 886 [M – ClO₄ – 3H₂O + 1, 100%]⁺, 863 [M – ClO₄ – 3H₂O – Na + 1, 15%]⁺. Analysis: C₅₄H₆₀ClN₈NaO₁₀ calculated, C 62.39, H 5.82, N 10.78; found, C 62.43, H 5.71, N 10.85%.

[La(H₃L)](ClO₄)₃·H₂O (**2**). A solution of **1** (0.21 g, 0.2 mmol) in acetonitrile (10 cm³) was added to a stirred solution of lanthanum perchlorate (0.22 g, ca 0.4 mmol) in acetonitrile (10 cm³) over 1 h. The reaction mixture was allowed to evaporate at room temperature for 1 week and yellow microcrystals of **2** were isolated, filtered off, washed with ethanol and dried over CaCl₂, yield 0.23 g (86% based on the cryptand). IR (KBr), $\nu = 3385w$, 3033, 2922, 2860, 1653vs(CN), 1541, 1477, 1452, 1350, 1296, 1221, 1146, 1221, 1146, 1115, 1088s (ClO₄), 768, 702 cm⁻¹; UV-Visible (acetonitrile), λ_{max} (log ϵ) = 293 (4.40), 415 (4.28); ¹H NMR (500 MHz, CD₃CN), $\delta = 12.81$ (br, 3 H, phenol-OH), 8.71 (d, 3 H, ³J_{HH} = 15.0, HC=N⁺), 8.50 (s, 3 H, HC=N), 8.20 [d, 3 H, Ph(1)-H(3), ⁴J_{HH} = 2.5 Hz], 8.02 [d, 3 H, Ph(1)-H(5), ⁴J_{HH} = 2.5 Hz], 7.69 [d, 6 H, ph(2)-H(2',6'), ³J_{HH} (2'3') = 8.0 Hz], 7.55 [t, 6 H, Ph(2)-H(3',5'), ³J_{HH} (2'3') = 8.0 Hz, ³J_{HH} (3'4') = 7.5 Hz], 7.44 [t, 3 H, Ph(2)-H(4'), ³J_{HH} (3'4') = 7.5 Hz], 4.052.78 (br, 24 H, CH₂CH₂), ¹³C NMR (CD₃CN), $\delta = 173.00$ (s, C=N⁺), 171.34 [s, Ph(1)-C(1)], 169.08 (s, C=N), 146.12 [s, Ph(1)-C(5)], 140.44 [s, Ph(1)-C(3)], 139.09 [s, Ph(2)-C(1)], 130.31 [s, Ph(2)-C(3',5')] 128.70 [s, Ph(2)-C(4')], 127.18 [s, Ph(1)-C(4)], 127.14 [m, Ph(2)-C(2',6') + Ph(1)-C(2), Ph(1)-C(6)], 61.87, 61.26, 60.76 (t, CH₂), 52.00 (s, CH₂N=); FAB-MS, m/z 1116 [M – 2HClO₄]⁺, 1100 [M – 2ClO₄ – H₂O]⁺, 1001 [M – 3ClO₄ – H₂O]⁺. Analysis: C₅₄H₅₆Cl₃LaN₈O₁₆ calculated, C 49.19, H 4.28, N 8.50; found, C 49.11, H 4.47, N, 8.78%.

[Eu(H₂L)(DMF)](ClO₄)₂·2H₂O·0.5Et₂O (**3**). A similar procedure to the above afforded **3** and **4**; yellow block crystals were obtained directly from the reaction by slow evaporation at room temperature, but the crystals very easily lose their crystalline solvents. To obtain more stable single crystals suitable for x-ray analysis, the reaction solution was mixed with a few drops of DMF. By slow diffusion of diethyl ether into the solution for 2 weeks at room temperature, yellow block crystals grew again, yield 74% IR (KBr), $\nu = 3419w$, 3064, 2925, 2861, 1652vs (CN), 1540, 1479, 1384, 1089s (ClO₄⁻), 842, 767, 698 cm⁻¹; UV-Visible (acetonitrile), λ_{max} (log ϵ) = 293 (4.45), 415 (4.29). Analysis: C₅₉H₆₉Cl₂EuN₉O_{14.5} calculated, C 52.14, H 5.12, N 9.28; found, C 52.01, H 5.25, N, 9.63%.

[Gd(H₂L)(DMF)](ClO₄)₂·6H₂O·0.5Et₂O (**4**). Yellow block crystals, yield 76%. IR (KBr); $\nu = 3415w$, 3116, 2927, 2865, 1652vs (CN), 1540, 1475, 1297, 1087s (ClO₄),

904, 771, 703 cm⁻¹; UV-visible (acetonitrile); λ_{max} (log ϵ) = 293 (4.42), 415 (4.29). Analysis: C₅₉H₇₇Cl₂GdN₉O_{18.5} calculated, C 49.69, H 5.46, N, 8.78; found C 49.69, H 5.46, N, 8.87%.

Supplementary data. Tables of atomic coordinates, bonds lengths and angles involving all the non-hydrogen atoms are deposited as supplementary data at the Cambridge Crystallographic Data Centre.

Acknowledgements

Financial support from the State Key Laboratories of Coordination Chemistry (Nanjing University, China) and Structural Chemistry (FJIRSM, China) is gratefully acknowledged. Dr S.-Y. Yu thanks Japan Society for the Promotion of Science for a postdoctoral fellowship.

REFERENCES

1. J.-M. Lehn. *Supramolecular Chemistry: Concepts and Perspectives*, Chapt. 8, pp. 89–138. VCH, Weinheim (1995).
2. M. Pietraszkiewicz. in *Comprehensive Supramolecular Chemistry*, edited by J.-M. Lehn, Vol. 10, edited by D. N. Reinhoudt, Chapt. 10, pp. 253–265. Pergamon Press, Oxford (1996).
3. J.-C. G. Bunzli. in *Lanthanide Probes in Life, Medical and Earth Sciences*, edited by G. R. Choppin and J.-C. G. Bunzli, Chapt. 7. Elsevier, Amsterdam (1989).
4. R. B. Lauffer. *Chem. Rev.* **87**, 901–927 (1987).
5. G. R. Choppin and K. M. Schaab. *Inorg. Chim. Acta* **252**, 299–310 (1996).
6. J. Rammo, R. Hettich, A. Roigk and H.-J. Schneider. *J. Chem. Soc., Chem. Commun.* 105–107 (1996).
7. K. G. Raganathan and H.-J. Schneider. *Angew. Chem. Int. Ed. Engl.* **35**, 1219–1221 (1996).
8. R. Häner, J. Hall and G. Rihs. *Helv. Chim. Acta*, **80**, 487–494 (1997).
9. S.-Y. Yu, S. Wang, Q.-H. Luo, L.-F. Wang, Z.-R. Peng and X. Gao. *Polyhedron* **12**, 1093–1096 (1993).
10. V. Alexander. *Chem. Rev.* **95**, 273–342 (1995).
11. S.-Y. Yu, Q. Huang, B. Wu, W.-J. Zhang and X.-T. Wu. *J. Chem. Soc., Dalton Trans.* 3883–3888 (1996).
12. S.-Y. Yu, Q.-M. Wang, B. Wu, X.-T. Wu, H.-M. Hu, L.-F. Wang and A.-X. Wu. *Polyhedron* **16**, 321–325 (1997).
13. A. W. Czarnik. *Acc. Chem. Res.* **27**, 302–308 (1994).
14. L. Fabbrizzi and A. Poggi. *Chem. Soc. Rev.* **24**, 197–202 (1995).
15. M. D. Timken, W. A. Marritt, D. N. Hendrickson, R. A. Gagne and E. Sinn. *Inorg. Chem.* **24**, 4202–4208 (1985).
16. F. Avecilla, R. Bastida, A. de Blas, D. E. Fenton, A. Macias, A. Rodriguez, T. Rodriguez-Blas, S. Garcia-Granda and R. Corzo-Suarez. *J. Chem. Soc., Dalton Trans.* 409–413 (1997).
17. J.-C. G. Bunzli, E. Moret, U. Casellato, P. Guerriero and P. A. Vigato. *Inorg. Chim. Acta* **150**, 133–139 (1988).
18. N. Sato, I. Yoshida and S. Shinkai. *Chem. Lett.* 1261–1264 (1993).
19. N. Sato, I. Yoshida and S. Shinkai. *J. Chem. Soc., Perkin Trans. 2* 621–624 (1993).
20. N. Sabbatini, M. Guardigli, A. Mecati, V. Balzani, R. Ungaro, E. Ghidini, A. Casnati and A. Pochini. *J. Chem. Soc., Chem. Commun.* 878–879 (1990).
21. W. D. Horrocks and D. R. Sudnick. *Acc. Chem. Res.* **14**, 384–392 (1981).
22. G. M. Sheldrick. *SADABS*. University of Göttingen, Göttingen (1996).
23. G. M. Sheldrick. *SHELXL-93: a Computer Program for Crystal Structure Refinement*. University of Göttingen, Göttingen, (1993).